VIP Molecular Dynamics Simulations

DOI: 10.1002/anie.200703987

Picosecond Melting of Ice by an Infrared Laser Pulse: A Simulation Study**

*Carl Caleman and David van der Spoel**

Hexagonal ice (Ih) is the most common form of ice, consisting of water molecules with their oxygen atoms arranged in a tetrahedral lattice. Both in the crystal and in the liquid form, oxygen atoms are spaced by 0.275 nm,[1] but the density of ice is 8% lower than that of water. This well-known property gives ice the ability to crack rocks or break a bottle of beer in the freezer. Each water molecule in ice forms four hydrogen bonds (two per molecule), and upon melting roughly 1.75 hydrogen bonds per water molecule are maintained. Ultrafast superheating and melting of bulk ice induced by infrared radiation was demonstrated recently using spectroscopy.[2] Herein, we describe the process of ice-melting using computer simulations of molecular dynamics (MD). MD simulations are ideally suited to investigate processes like melting and freezing, as they allow us to simultaneously probe the structure and dynamics of the system under investigation at atomic resolution and on a femtosecond time scale.

To describe the thermal melting of ice, ionization processes have to be avoided. In practice, this means that the amplitude of the pump laser should be low enough that multiphoton or field ionization processes are avoided, and the photon energy should be kept under the single-photon ionization threshold, that is, $\lambda > 140$ nm.[3,4] As a rough guideline for the laser intensity, we used $I\lambda^2 < 10^6$ W,[5] where λ is the wavelength of light and I is the power by area given by $I = cE_0^2 \in_0/2$, where c is the speed of light, E_0 the maximum amplitude of the electric field, and $\in_0$ the permittivity of vacuum. Under these circumstances, the ionization probability is negligible. At room temperature the frequency of the molecular vibrations of water are comparable to kT, and in thermal equilibrium the molecules are primarily in the ground state. To consider non-equilibrium processes, such as vibration–relaxation, a quantum-mechanical description is desirable.[6] However, accurate time-dependent quantum calculations for large systems, such as the system studied herein, are not tractable. Therefore, in practice, a classical description augmented by quantum corrections is adopted[7] for such calculations. The flexible water model used throughout this work (flexible TIP4P[6]) includes a Morse potential for the OH bonds, an anharmonic coupling term between bond stretches, and a coupling between bond stretching and angle bending, which makes it suitable for simulating absorption of infrared radiation. The model has been shown to reproduce density, energy, and vibration spectra of liquid water. It also reproduces the red shift in the vibration spectra in liquid D_2O by changing the weight of the hydrogen atoms.[6] The model has also been employed to calculate the vibration lifetime of HDO in D_2O.[8]

The wavelength of the laser λ was limited to $2.0 < \lambda < 4.0$ μm, corresponding to the symmetric and asymmetric stretch of water around the absorption maximum of ice Ih.[2,9] The GROMACS molecular dynamics package[10] was extended to include a pulsed, time-dependent electric field [Eq. (1) and Figure 1a; σ is the pulse width, and t is the time after the pulse maximum at t_0].

$$E(t) = E_0 \exp[-\frac{(t-t_0)^2}{2\sigma^2}]\cos[\omega(t-t_0)] \quad (1)$$

The angular frequency $\omega = 2\pi c/\lambda$ was varied in the infrared (IR) regime as described above. Two different intensity/pulse width combinations were used: $E_0 = 2.5\ \mathrm{V\,nm^{-1}}$, $\sigma = 100$ fs or $E_0 = 1.0\ \mathrm{V\,nm^{-1}}$, $\sigma = 1$ ps. Unless

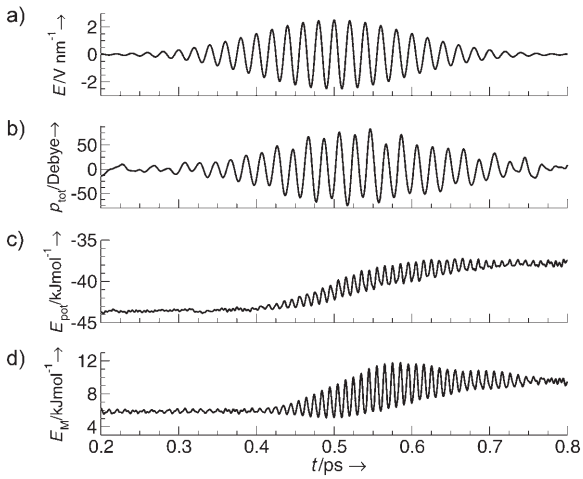

Figure 1. Simulation of an ice crystal with $E_0 = 2.5\ \mathrm{V\,nm^{-1}}$, $\sigma = 100$ fs, $t_0 = 0.5$ ps, $\lambda = 3.0$ μm, $T_{start} = 250$ K. a) Amplitude of the applied electric field. b) The total dipole moment of the simulation box in the direction of the applied field clearly follows the applied field. c) Potential energy and d) Morse (bond) energy.

[*] Dr. C. Caleman, Dr. D. van der Spoel
Department of Cell and Molecular Biology
Biomedical Centre, Uppsala University
Box 596, 75124 Uppsala (Sweden)
Fax: (+46) 185-117-55
E-mail: spoel@xray.bmc.uu.se

[**] Stimulating discussions with Jörgen Larsson, Abraham Szöke, Klas Andersson, Magnus Bergh, Anne L'Huillier, Richard London, Gösta Huldt, and Janos Hajdu are gratefully acknowledged. Many thanks to Martin Chaplin for his supportive webpage: http://www.lsbu.ac.uk/water/. The Swedish Research Foundation is acknowledged for financial support.

Supporting information for this article is available on the WWW under http://www.angewandte.org or from the author.

otherwise noted, all simulations started at a temperature $T_{start} = 250$ K. The starting structure used for the simulations was a solid crystal of 768 molecules.[11] A discussion of the effect of periodic boundary conditions on the electric field is given in the Supporting Information. Further simulation details are given in reference [12].

In an oscillating electric field with a frequency of 100 THz ($\lambda = 3.0$ μm) the dipole moment p_{tot} of an ice cube will follow the applied electric field, but its magnitude will not surpass 80 Debye for the system studied (Figure 1b), or, in other words, $p \approx 0.1$ Debye molecule^{-1}, which is roughly 4–6% of the molecular dipole (depending on which reference value is used). In contrast, in a constant electric field the total dipole of the system is linearly dependent on the electric field for low field strengths (see Figure S1 in the Supporting Information). The potential energy increases quickly during and (slightly) after the pulse (Figure 1c), and the main component responsible for this rise is the increased bond energy (Figure 1d), showing that the field energy is transferred primarily to the OH bonds. The potential energy oscillates at double the frequency of the external field (Figure 1c), owing to the fact that the potential energy absorbed in a bond is positive both for stretching and compressing the bond, or, in other words that $E_{abs} \sim I^2$. Interestingly, the peaks in the dipole p_{tot} and in the energy terms are roughly 7 fs after the peak in the field, corresponding to a phase difference of approximately 120°. The reason for this delay is that the dipole moment continues to increase while the field has the same direction but stops when the field is not sufficiently strong to increase the length of the bonds any further.

Absorption is wavelength-dependent. Figure 2 shows properties of a system subjected to fields with $\lambda = 3.0$ μm and $\lambda = 2.85$ μm. The peak in the absorption spectrum is at $\lambda =$ 3.0 μm (see Figure S2 in the Supporting Information), and at this laser wavelength ice melts readily, whereas it does not melt as easily at $\lambda = 2.85$ μm. At $\lambda = 3.0$ μm, 10 kJ mol^{-1} is absorbed versus only 4 kJ mol^{-1} at $\lambda = 2.85$ μm. In the latter case the potential energy increases by roughly 2 kJ mol^{-1} (Figure 2b) during the pulse, and the remaining energy absorbed by the crystal is put into heating (Figure 2c), which corresponds to a temperature increase of 45 K. The total energy is constant before and after the pulse (Figure 2a). The difference between melting ($\lambda = 3.0$ μm) and superheating ($\lambda = 2.85$ μm) is obvious from the number of hydrogen bonds (HB) per molecule (Figure 2e). In the superheated system, the number of HB is constant at the ice level, whereas it is reduced by 12% in the melted system. The potential energy increase of 2 kJ mol^{-1} in the superheated system therefore goes predominantly into excitation of the intramolecular degrees of freedom. On longer time scales the energy absorbed in the bonds in the melting system will make the molecules drift and rotate out of their positions, which causes breaking of the hydrogen bonds (Figure 2e), and kinetic energy is transferred to potential energy, that is, increased potential energy and a cooler system.

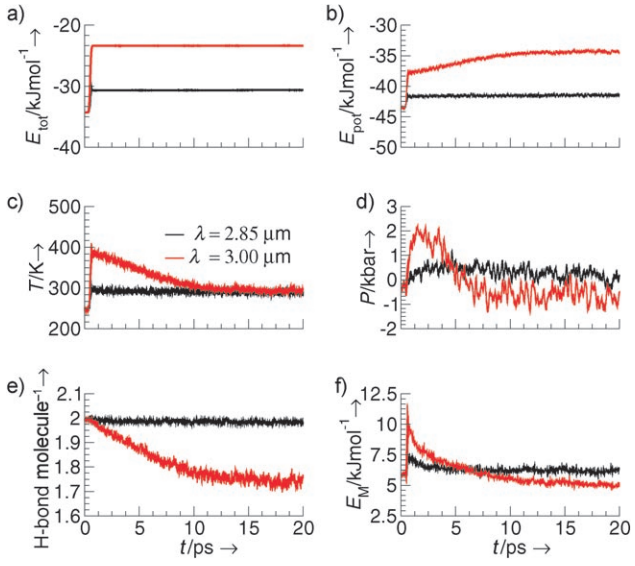

Figure 2. Solid ice crystal at $E_0 = 2.5$ V nm^{-1}, $\sigma = 100$ fs, $t_0 = 0.5$ ps, $\lambda = 3.0$ μm (red, showing an example of a system that melts) and $\lambda = 2.85$ μm (black, showing a typical superheated system). a) total energy, b) potential energy, c) temperature, d) pressure, e) number of hydrogen bonds, f) Morse (bond) energy as a function of time. For clarity, the curves in (d) are presented as a running average over 125 fs.

The pressure in the superheated system increases to 400 bar (Figure 2d), mainly owing to the higher temperature. For a system that is heated sufficiently to melt, the pressure reaches as high as 2 kbar a few picoseconds after the pulse, but once the pressure goes down again, after around 5 ps, it equilibrates to a value below the starting pressure in the crystalline phase. This behavior is a clear indication that the system melts, since the density of the liquid is higher than the solid and hence a small void is formed. Negative pressure in a simulation indicates that the system wants to contract, to fill the void and minimize the corresponding surface area.[13] In a simulation aimed at exactly reproducing the conditions of the experiments of Iglev et al.[2] ($\sigma = 1.0$ ps, $\lambda = 2.8$ μm, and $E_0 =$ 1.0 V nm^{-1}), we observe a temperature increase of 20 K and a pressure increase of around 300 bar (not shown), in good agreement with the data.

The time evolution of a typical system that melts is shown in Figure 3. During the pulse the temperature increases by 150 K, just after the peak in the laser pulse. This kinetic energy leads to an initiation of melting after a few picoseconds. Melting implies an increase in potential energy, and hence a decrease in temperature. After 15 to 20 ps the ice has melted completely. The melting process seems to follow a nucleation process, in which the breaking of the hydrogen bonds starts at a very localized position ("melt seed" in Figure 3) and spreads from there. The ice structure can locally stay intact a couple of picoseconds after the melting process is initiated (see "ice core" in Figure 3). This melting process is very similar to the (time-reverse of the) freezing of water described by Matsumoto et al.,[14] who showed that freezing is a rare process starting from a nucleation core.

Recent experimental studies (using ultrafast infrared spectroscopy) of structural dynamics in liquid water induced by an infrared laser (pumping the intramolecular bonds) demonstrated that the structural response follows a two-stage mechanism. The energy from the laser is first absorbed into intramolecular vibrations in the excited molecules and then

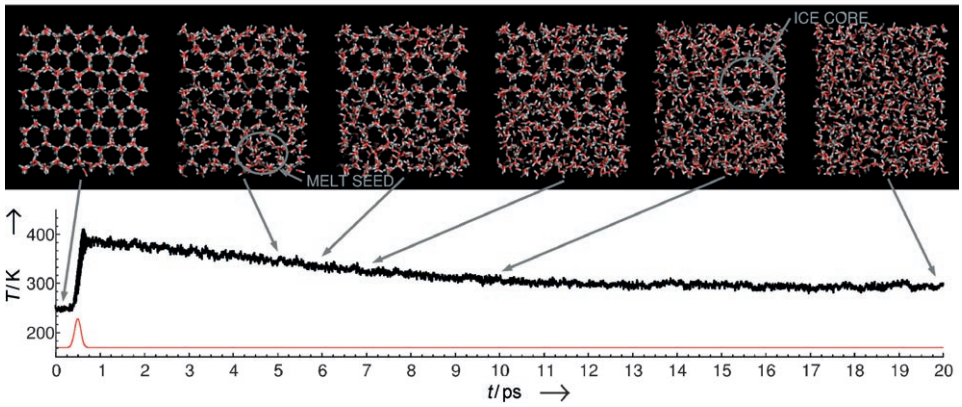

Figure 3. Snapshots of the trajectory of an ice crystal and the temperature as a function of time. The pulse envelope is drawn schematically in red. ($E_0 = 2.5\ \mathrm{V\,nm^{-1}}$, $\sigma = 100$ fs, $t_0 = 0.5$ ps, $\lambda = 3.0$ μm, $T_{start} = 250$ K).

transferred into the intermolecular network, resulting in a weakening of hydrogen bonds.[15] Furthermore, the energy delocalization over many molecules was found to occur on a 1-ps time scale, thus resulting in a macroscopically heated sample. The time scale of this process is determined by the molecular reorientation and the change of the hydrogen bond length.[16] By monitoring the vibrational, rotational, and translational energies in our systems, we have made a detailed study of the energy transfer within the ice crystal (Figure 4). Before the pulse the velocities follow a Maxwell distribution, equally divided between rotational, vibrational, and translational energy. The laser pulse pumps the OH bonds in the molecules uniformly throughout the system. After the laser pulse, three different steps can be identified (Figure 4): 1) Intramolecular OH bonds are excited; the vibrational energy reaches its peak just after the laser pulse. 2) Around 1 ps after the laser pulse, the vibrational energy and the rotational energy of the molecules (predominantly librational energy) have equilibrated. 3) At 3–6 ps after the laser pulse, the energy is again evenly spread out, and the equipartition theorem is no longer violated. The gain in translational energy is directly related to the breakdown of the crystal structure. With a higher kinetic energy, the probability of a molecule breaking out of the crystal lattice increases. Once the symmetry is broken, the probability for the surrounding molecules to "melt" increases further, owing to the defect in the crystal. Previous simulations indicated that topological effects, in which five- and seven-membered (rather than six-membered) rings are formed, play an important role in the bulk melting of ice.[17] Melting obviously depends on the temperature and the structure of the system. A crystal can stay superheated for nanoseconds, until a melt seed forms, after which molecules next to the melt seed start to melt as well, following a roughly exponential decay of the number of hydrogen bonds (Figure 2e). A hydrogen-bond analysis based on a different wavelength shows virtually identical relaxation. Because of the lattice, the overall relaxation takes slightly longer in ice than in water.[15]

The effect of wavelength, and hence the amount of absorbed energy, on the melting process is depicted in Figure 5a. At $\lambda = 2895$ nm the temperature increases to almost 350 K and melting is a rapid process. At a slightly shorter wavelength ($\lambda = 2855$ nm), the ice is metastable for more than 500 ps. To quantify the kinetics of the melting process, we define a characteristic melting time τ_{melt} as the time at which the number of hydrogen bonds (N_{HB}) is halfway between the amounts in ice at 250 K and in water at the temperature of the system once it reaches equilibrium, which depends on the amount of energy absorbed and the starting temperature. For example, in the case of Figure 2e this implies $N_{HB} = 1.86$ and $\tau_{melt} = 5.8$ ps. Figure 5b shows τ_{melt} for more than 150 simulations of 2 ns each, with two different

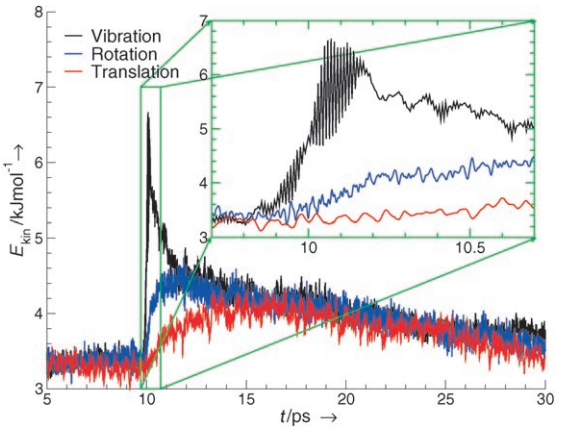

Figure 4. Distribution of kinetic energy in ice, over vibrational, rotational (including libration) and translational degrees of freedom during a laser pulse with $E_0 = 2.5\ \mathrm{V\,nm^{-1}}$, $\sigma = 100$ fs, $t_0 = 10$ ps, $\lambda = 2.9$ μm, $T_{start} = 270$ K. The inset shows clearly that the equipartition theorem is violated during the pulse. Redistribution of kinetic energy over the components of the kinetic energy takes 5–6 ps.

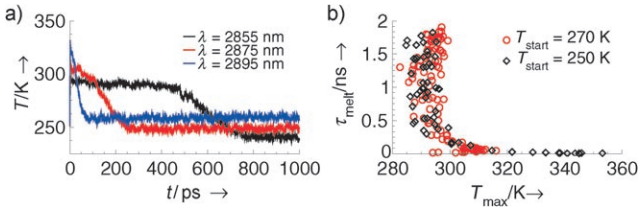

Figure 5. a) Temperature as a function of time for three different absorptions. b) 50% melt time (defined in the text) as a function of the maximum temperature T_{max} reached in the sample for two different starting temperatures T_{start}. The pulse parameters were $E_0 = 2.5\ \mathrm{V\,nm^{-1}}$, $\sigma = 100$ fs, $T_{start} = 250$ K for the simulations in (a). In (b), simulations under the same conditions were used, plus additional simulations with $E_0 = 0.5\ \mathrm{V\,nm^{-1}}$, $\sigma = 1.0$ ps, and $T_{start} = 270$ K. For clarity the curves in (a) are presented as a running average over 500 fs. Each symbol in (b) represents a 2-ns simulation with different λ leading to different T_{max}.

starting temperatures T_{start}. Obviously, the kinetics of the phase transition from ice to liquid water induced by femtosecond IR lasers is dependent on the maximum temperature reached by the ice, T_{max}, just after the laser pulse, and the starting temperature does not affect τ_{melt} at all. A system heated to a temperature above 290 K will melt within approximately 50 ps, whereas a system heated to a temperature below 290 K can stay superheated for hundreds of picoseconds (Figure 5b). Recent experimental results, presented by Schmeisser et al.[18] have shown that there is a temperature limit for superheating of bulk ice at 330 ± 10 K. Taking into account that the equilibrium melting temperature for the water model used herein is around 30–40 K[19] too low, our results agree well with the experimental ones. We find that exciting the system to a temperature lower than 280 K results in a superheated system that does not melt to 50% within 2 ns (i.e. $\tau_{melt} > 2$ ns, Figure 5b), in good agreement with earlier Monte Carlo calculations, showing that hexagonal ice is metastable up to a temperature of around 300 K.[20] Finally, superheated ice structures are present even when heating to much higher temperatures, but on a much shorter time scale (Figures 3 and 5a).

Herein, we have demonstrated that thermal melting of ice follows a nucleation process that starts locally and then spreads throughout the crystal. The time scale for melting depends on how much energy is put in. For $T_{max} > 290$ K, melting happens within a few picoseconds; for lower T_{max}, superheated ice is significantly more stable. Redistribution of kinetic energy over degrees of freedom after the laser pulse proceeds in two steps and takes 3–6 ps.

Received: August 30, 2007
Revised: October 23, 2007
Published online: January 4, 2008

Keywords: ice · infrared radiation · laser heating · molecular dynamics · phase transitions

[1] W. F. Kuhs, M. S. Lehmann, *J. Phys.* **1987**, *48*, 3.
[2] H. Iglev, M. Schmeisser, K. Simeonidis, A. Thaller, A. Laubereau, *Nature* **2006**, *439*, 183.
[3] B. Winter, M. Faubel, *Chem. Rev.* **2006**, *106*, 1176.
[4] J.-H. Guo, Y. Luo, A. Augustsson, J.-E. Rubensson, C. Såthe, H. Ågren, H. Siegbahn, J. Nordgren, *Phys. Rev. Lett.* **2002**, *89*, 137402.
[5] G. Mainfray, C. Manus, *Rep. Prog. Phys.* **1991**, *54*, 1333.
[6] C. P. Lawrence, J. L. Skinner, *Chem. Phys. Lett.* **2003**, *372*, 842.
[7] S. A. Egorov, K. F. Everitt, J. L. Skinner, *J. Phys. Chem. A* **1999**, *103*, 9494.
[8] C. P. Lawrence, J. L. Skinner, *J. Chem. Phys.* **2003**, *119*, 1623.
[9] G. M. Hale, M. R. Querry, *Appl. Opt.* **1973**, *12*, 555.
[10] D. van der Spoel, E. Lindahl, B. Hess, G. Groenhof, A. E. Mark, H. J. C. Berendsen, *J. Comput. Chem.* **2005**, *26*, 1701.
[11] J. A. Hayward, J. R. Reimers, *J. Chem. Phys.* **1997**, *106*, 1518.
[12] The particle mesh Ewald[21] (PME) method was used to model long-range electrostatic interactions. An integration step of 0.2 fs was used in the simulations which were 30–2000 ps in length, total. Simulations at the two different intensity/pulse width combinations defined in the text were done with wavelengths from 2.0 μm to 4.0 μm spaced 50 nm; one to three simulations where made at every wavelength. The total energy was verified to be conserved such that $\Delta E_{tot}/E_{tot} < 0.02$ after 1 ns.
[13] D. van der Spoel, E. J. W. Wensink, A. C. Hoffmann, *Langmuir* **2006**, *22*, 5666.
[14] M. Matsumoto, S. Saito, I. Ohmine, *Nature* **2002**, *416*, 409.
[15] S. Ashihara, N. Huse, A. Espagne, E. T. J. Nibbering, T. Elsaesser, *J. Phys. Chem. A* **2007**, *111*, 743.
[16] D. Laage, J. T. Hynes, *Science* **2006**, *311*, 832.
[17] D. Donadio, P. Raiteri, M. Parrinello, *J. Phys. Chem. B* **2005**, *109*, 5421.
[18] M. Schmeisser, H. Iglev, A. Laubereau, *Chem. Phys. Lett.* **2007**, *442*, 17.
[19] C. Vega, E. Sanz, J. L. F. Abascal, *J. Chem. Phys.* **2005**, *122*, 114507.
[20] C. McBride, C. Vega, E. Sanz, L. G. MacDowell, J. L. F. Abascal, *Mol. Phys.* **2005**, *103*, 1.
[21] U. Essmann, L. Perera, M. L. Berkowitz, T. Darden, H. Lee, L. G. Pedersen, *J. Chem. Phys.* **1995**, *103*, 8577.

